

A Detailed Study on the Equal Arrival Time Surface Effect in Gamma-Ray Burst Afterglows*

Yong-Feng Huang^{1,2}, Ye Lu^{2,3}, Anna Yuen Lam Wong² and Kwong Sang Cheng²

¹ Department of Astronomy, Nanjing University, Nanjing 210093; hyf@nju.edu.cn

² Department of Physics, The University of Hong Kong, Pokfulam Road, Hong Kong

³ National Astronomical Observatories, Chinese Academy of Sciences, Beijing 100012

Received 2006 August 15; accepted 2006 October 21

Abstract Due to the relativistic motion of gamma-ray burst remnant and its deceleration in the circumburst medium, the equal arrival time surfaces at any moment are not spherical, rather, they are distorted ellipsoids. This will leave some imprints in the afterglows. We study the effect of equal arrival time surfaces numerically for various circumstances, i.e., isotropic fireballs, collimated jets, density jumps and energy injection events. For each case, a direct comparison is made between including and not including the effect. For isotropic fireballs and jets viewed on axis, the effect slightly hardens the spectra and postpones the peak time of the afterglows, but does not change the shapes of the spectra and light curves significantly. In the cases of a density jump or an energy injection, the effect smears out the variations in the afterglows markedly.

Key words: gamma rays: bursts — relativity — shock waves — ISM: clouds

1 INTRODUCTION

Afterglow observations have made it clear that gamma-ray bursts (GRBs), both long and short, typically lie at cosmological distances (Costa et al. 1997; Frail et al. 1997; Galama et al. 1997; Vreeswijk et al. 1999; Hjorth et al. 2002; Villasenor et al. 2005; Fox et al. 2005), with the highest redshift recorded so far at $z \sim 6.3$ for GRB 050904 (Tagliaferri et al. 2005; Haislip et al. 2006; Price et al. 2006; Watson et al. 2006; Cusumano et al. 2006). Evidence is also accumulating that supports the idea that long/soft GRBs may come from the collapse of massive stars, while short/hard GRBs come from the merger of two compact objects (Barthelmy et al. 2005). As the most violent bursts in the Universe since the Big Bang, GRBs and their afterglows can be satisfactorily understood in the framework of the relativistic fireball model, which postulates that the main burst emission should be due to internal shocks and the afterglow emission can be accounted for by external shocks (Mészáros & Rees 1992, 1997; Sari, Narayan & Piran 1996; Vietri 1997; Wijers, Rees & Mészáros 1997; Sari, Piran & Narayan 1998; Dermer, Chiang & Böttcher 1999; Su et al. 2006; and for recent reviews, see: van Paradijs, Kouveliotou & Wijers 2000; Piran 2004; Zhang & Mészáros 2004; Zhang 2007).

GRBs are one of the most relativistic phenomena in our cosmos. The initial bulk Lorentz factor of GRB ejecta can be as high as 100–1000. Such an ultra-relativistic motion induces two effects on the afterglows. First, the emission is strongly enhanced in the direction of motion due to relativistic boosting. Secondly, photons emitted simultaneously from a spherical surface of the GRB remnant do not reach the observer at the same time. Photons at higher latitude will arrive later. In other words, at any lab-frame time, while the shape of the GRB remnant itself is spherical, the photons received by the observer actually do not come

* Supported by the National Natural Science Foundation of China.

from a spherical surface, but from a distorted ellipsoid, i.e., the equal arrival time surface (Waxman 1997; Panaitescu & Mészáros 1998; Sari 1998; Granot, Piran & Sari 1999; Gao & Huang 2006). Additionally, if angularly resolved by a telescope, the equal arrival time surface (EATS) would not be homogeneous in brightness, but would show a ring-like structure.

Exact analytical expressions for the geometric shape of EATS can be derived under some simplifying assumptions in the ultra-relativistic stage, for example, in the cases of fully radiative and adiabatic regimes (Bianco & Ruffini 2005), but the effect of EATS on the emission can be well incorporated in the modeling of GRB afterglows only through numerical calculations. This has been done by a few authors (Panaitescu & Mészáros 1999; Moderski, Sikora & Bulik 2000; Huang et al. 2000a, b; Salmonson 2003; Kumar & Granot 2003; Granot 2005). However, a direct comparison between including and not including the effect of EATS, which can reveal the effect more clearly, is still lacking. In this article, we intend to carry out such a comparison. This paper is organized as follows. We describe our model in Section 2. The numerical results are then presented in Section 3 under various conditions including isotropic fireballs, jets, energy injections, and density variations in the circumburst medium. Finally, Section 4 gives our conclusions and a discussion.

2 MODEL DESCRIPTION

According to the standard fireball theory, afterglows are produced when the GRB ejecta, either isotropic or highly collimated, plough through the circumburst medium, producing a strong blastwave that accelerates the swept-up electrons. Synchrotron emission from these electrons is the dominant radiation mechanism that takes place in the afterglow stage, although inverse Compton scattering may also play a role in some cases (Wei & Lu 2000; Sari & Esin 2001). The GRB ejecta are initially ultra-relativistic, but may become trans-relativistic in a few months (Huang et al. 1998), and enter the deep Newtonian phase after two or three years (Huang & Cheng 2003). Additionally, the blastwave is in the highly radiative regime in the first few hours, and is adiabatic thereafter.

A simple model that can realistically depict the overall evolution of GRB afterglows and which lends itself to easy numerical solution has been proposed by Huang et al. (1999, 2000a,b), Huang & Cheng (2003). We will use this model for the current study. Now we first describe the model briefly for completeness. In the description below, unless declared explicitly, physical quantities are all measured in the observer's static lab frame.

The model is mainly characterized by a generic dynamical equation of (Huang et al. 1999),

$$\frac{d\gamma}{dm} = -\frac{\gamma^2 - 1}{M_{\text{ej}} + \epsilon m + 2(1 - \epsilon)\gamma m}, \quad (1)$$

where γ is the bulk Lorentz factor of the shocked medium, m is the swept-up mass, M_{ej} is the initial mass of the GRB ejecta, and ϵ is the radiative efficiency. Equation (1) is applicable in both the ultra-relativistic and the non-relativistic phases (Huang et al. 1999). For collimated GRB ejecta, the lateral expansion is described realistically by (Huang et al. 2000a,b),

$$\frac{d\theta}{dt} = \frac{c_s(\gamma + \sqrt{\gamma^2 - 1})}{R}, \quad (2)$$

where θ is the half-opening angle of the jet, R the radius of the shock, t the observer's time, and c_s the comoving sound speed given by

$$c_s^2 = \hat{\gamma}(\hat{\gamma} - 1)(\gamma - 1) \frac{1}{1 + \hat{\gamma}(\gamma - 1)} c^2, \quad (3)$$

with $\hat{\gamma} \approx (4\gamma + 1)/(3\gamma)$ being the adiabatic index.

In the calculation of the synchrotron radiation from the shock-accelerated electrons, the electron distribution function is a key factor. Basically the electrons follow a power-law distribution in energy, with a power-law index p typically ranging between 2 and 3. Here we adopt a refined function that takes into account the cooling effect (Dai, Huang & Lu 1999; Huang & Cheng 2003). Note that our distribution function

is applicable even in the deep Newtonian phase (Huang & Cheng 2003). As usual, we denote the energy ratios of electrons and magnetic field to protons by ξ_e and ξ_B , respectively.

In order to include the EATS effect, the observed afterglow flux density at any given time t should be calculated by integrating over the EATS determined by

$$\int \frac{1 - \beta \cos \Theta}{\beta c} dR \equiv t, \quad (4)$$

within the ejecta boundaries (Moderski et al. 2000), where $\beta = \sqrt{\gamma^2 - 1}/\gamma$ and Θ is the latitude angle on the EATS. In our model, it is also very easy to remove the consideration on EATS, so that we can clearly see how the EATS affects the GRB afterglow. For details on how to calculate the dynamics and the radiation process, readers may refer to Huang et al. (1999, 2000a,b) and Huang & Cheng (2003).

3 NUMERICAL RESULTS

In this section, we use our model to investigate the EATS effect in GRB afterglows under various conditions. For each condition, we will directly compare the two instances where the EATS effect is and is not included. For convenience, we first define a set of “standard” parameters that will be generally used in our calculations: $\xi_e = 0.1$, $\xi_B = 0.001$, $p = 2.5$, the isotropic equivalent energy of the GRB ejecta $E_{0,\text{iso}} = 10^{53}$ erg, the initial Lorentz factor $\gamma_0 = 300$, the number density of the circumburst medium $n = 1 \text{ cm}^{-3}$, and the luminosity distance of the GRB $D_L = 1 \text{ Gpc}$. For the jets, we take the initial half-opening angle as $\theta_0 = 0.1$. These parameter values are quite typical in GRB afterglows.

3.1 Isotropic Fireballs

In Figure 1, we illustrate the evolution of the afterglow spectrum for an isotropic fireball with “standard” parameters. The solid lines correspond to the instance when the EATS effect is included, while the dashed lines correspond to the case when the EATS effect is omitted. A few interesting features can be clearly seen from this figure. First, the spectrum at any particular moment can be divided into three segments. Taking the spectrum at $t = 10^5$ s as an example, the three segments are approximately $S_\nu \propto \nu^{0.34}$, $\nu^{-0.76}$ and $\nu^{-1.27}$. They are in good agreement with theoretical expectations, i.e., $S_\nu \propto \nu^{1/3}$, $\nu^{(1-p)/2}$ and $\nu^{-p/2}$ (Sari, Piran & Narayan 1998). Note that the EATS does not change the slope of each segment. Secondly, the peak flux density ($S_{\nu,\text{max}}$) does not change significantly with time. This is true irrespective of the EATS consideration. However, the inclusion of the EATS does reduce the peak frequency, $S_{\nu,\text{max}}$, by a factor of ~ 2 . Thirdly, the EATS effect makes the spectrum slightly harder. As a result, the peak frequency ν_{max} (corresponding to $S_{\nu,\text{max}}$) is made slightly higher, reducing the emission below ν_{max} while enhancing that above ν_{max} . This effect is easy to understand. On an EATS, the material at high latitude actually corresponds to an earlier stage of the ejecta shell, which has a larger Lorentz factor and naturally emits harder photons. Additionally, electrons enclosed in an EATS is fewer in number than those in the corresponding sphere. This is the reason of the reduction of $S_{\nu,\text{max}}$ mentioned above.

Finally, we also note that the EATS effect is less significant at very high frequencies. For example, there is little difference between the solid line and its corresponding dashed line when $\nu \geq 10^{17}$ Hz. This can also be easily understood. High energy photons are mostly emitted by high speed materials, which mainly reside at the top point of the EATS and whose emission is restricted within a small solid angle due to relativistic beaming effect. In other words, high energy photons are emitted from a small portion of the EATS which is at the top point and differs from a sphere marginally.

Figure 2 shows the EATS effect on the R -band afterglow light curve. An obvious feature is that the EATS effect postpones the peak time (t_{peak}) of the optical afterglow by a factor of ~ 2 . Also, before the peak time, the EATS effect makes the afterglow dimmer, but after the peak time, it makes the afterglow slightly brighter. However, the EATS effect does not alter the slopes of the light curve, either before or after the peak time. Figure 3 illustrates the EATS effect on the X-ray afterglow. While the basic features of Figure 3 are generally similar to those of Figure 2, an obvious difference is that the dimming and brightening of X-ray emission before and after the peak time due to the EATS effect is much weaker. It is consistent with the spectral characteristics revealed in Figure 1.

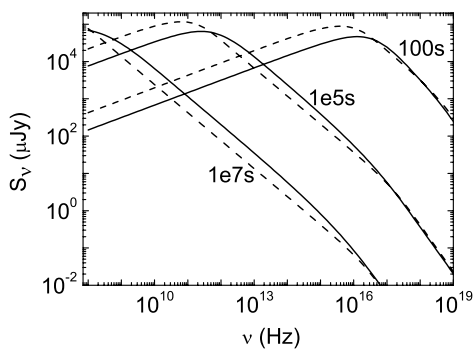


Fig. 1 Spectrum evolution of an isotropic fireball with “standard” parameters. The solid lines are drawn with the EATS effect included. As a comparison, the dashed lines do not incorporate the EATS effect. The number near each pair of curves indicates the time at which the spectra are sampled.

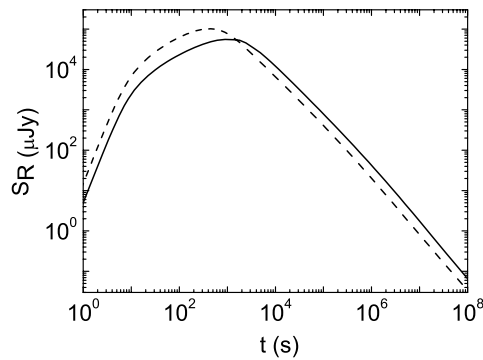


Fig. 2 *R*-band afterglow light curves of an isotropic fireball. Line styles and parameters are the same as in Fig. 1.

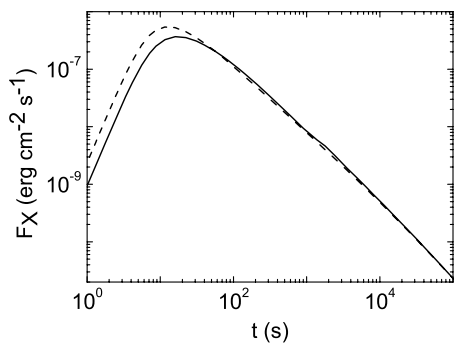


Fig. 3 0.1–10 keV X-ray afterglow light curves of an isotropic fireball. Line styles and parameters are the same as in Fig. 1.

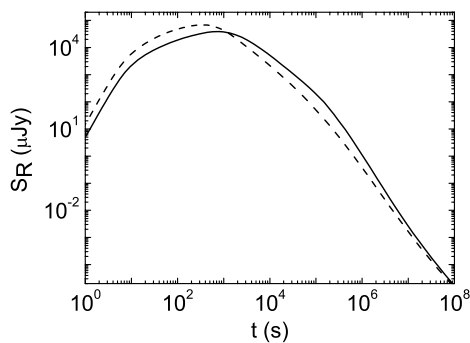


Fig. 4 *R*-band afterglow light curves of a jet with “standard” parameters. The solid line is drawn with the EATS effect included, while the dashed line is drawn with the effect excluded.

3.2 Jets

The EATS effect on the optical afterglow of jets is illustrated in Figure 4. Generally speaking, the role played by the EATS on jets is quite similar to that on isotropic fireballs, i.e., postponing the peak time, reducing the brightness before t_{peak} , and enhancing it after t_{peak} .

Figure 5 shows the afterglow light curves when the observer is off-axis. An obvious feature can be immediately noted in this figure that the dashed line is much higher above the solid line when $t < t_{\text{peak}}$. This behavior is not completely unexpected. As we know, when an observer is off-axis, the observed flux will be very low due to relativistic beaming. Taking EATS into account, high latitude photons actually come from material with larger Lorentz factors, which means the beaming effect is more serious. The effect is especially notable at early stages ($t < t_{\text{peak}}$), when the decrease of the Lorentz factor of the jet is extremely rapid.

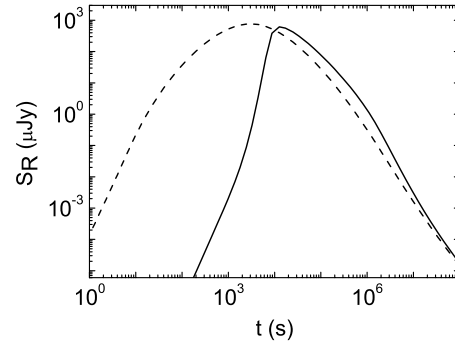


Fig. 5 *R*-band afterglow light curves of a jet with “standard” parameters, but viewed at an angle of 0.17. Line styles are the same as in Fig. 4.

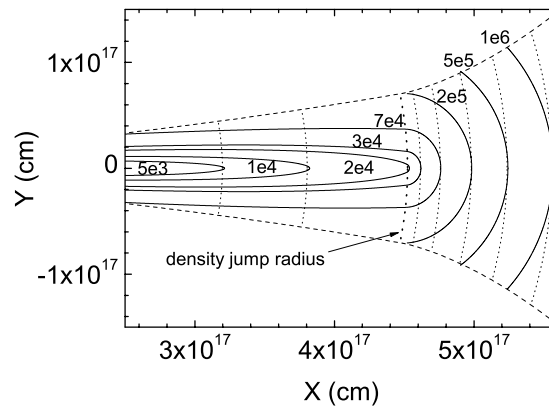


Fig. 6 Exemplar surfaces of equal arrival times for a “standard” jet encountering a density jump at $t = 2 \times 10^4$ s. The amplitude of the density jump is 100 times. X -axis is the direction of motion of the jet, and Y -axis is the lateral direction. The solid lines illustrate the equal arrival time surfaces, with the time marked in unit of s. The dotted lines show the corresponding spherical surfaces. The dashed lines are jet boundaries.

3.3 Density Jump Cases

When the GRB ejecta encounter a sudden density increase in the circumburst medium, a rebrightening of the afterglow will be observed (Lazzati et al. 2002; Nakar & Piran 2003; Dai & Wu 2003; Tam et al. 2005). It would be of interest to investigate how the EATS takes effect when such a brightness variation is involved. Here we assume that the number density of the circumburst medium jumps suddenly from 1 cm^{-3} to 100 cm^{-3} at the observer’s time 2×10^4 s (corresponding to a radius of $R_J \sim 4.5 \times 10^{17}$ cm). The numerical results are presented in Figures 6 – 7.

Figure 6 shows a few surfaces of equal arrival times, compared directly with the spherical geometry of the jet. At early stages, when the jet is still highly ultra-relativistic, the EATSs are very flat and deviate greatly from spherical surfaces. However, it is interesting to note that the foreland of the EATS becomes more round when $R > R_J$. This is because the jet decelerates rapidly after the density jump, making the relativistic effect less significant. At time 10^6 s, when the Lorentz factor of the jet is $\gamma \sim 1.2$, the EATS no longer deviates markedly from a sphere. In our calculations, when the blastwave reaches the density jump radius, its Lorentz factor is $\gamma \approx 9$. Thus the EATS will completely pass through the density jump surface in a time of $R_J/\gamma^2 c \sim 1.9 \times 10^5$ s. This can also be clearly seen in Figure 6.

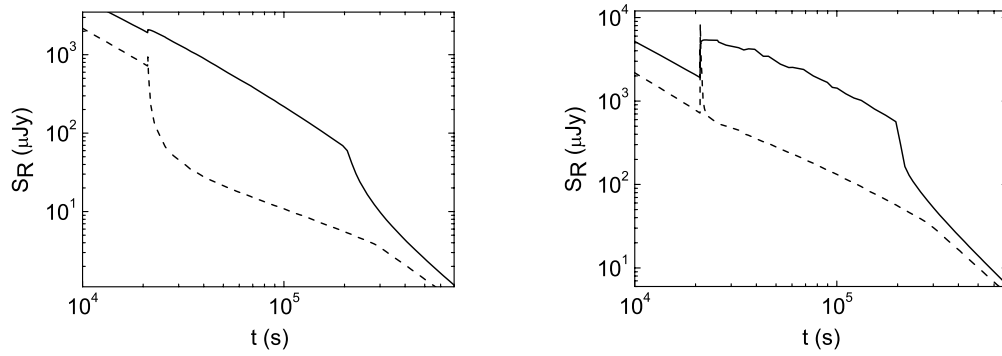


Fig. 7 (a) *R*-band afterglow light curves of a jet encountering a density jump at $t = 2 \times 10^4$ s. The amplitude of the density jump is 100 times. Other parameters involved are the same as in Fig. 4. The solid line and the dashed line correspond respectively to the instances when the EATS effect is and is not included. (b) Same as (a), except that ξ_B increases by a factor of 50 simultaneously at the jump radius.

Figure 7 shows the *R*-band afterglow light curves. The dashed line in Figure 7a corresponds to the instance where the EATS effect is not considered. We see that a sharp rebrightening does appear at the density jump moment. However, the flux density decreases steeply soon after the density jump. This is mainly due to the rapid deceleration of the blastwave in the much denser environment. When the EATS effect is included in our calculation, the rapid variation is largely smeared out, resulting in a very different light curve (the solid line). First, the rapid decline of the brightness seen at $t > 2 \times 10^4$ s in the dashed line is now postponed to $\sim 2 \times 10^5$ s. This is easy to understand. We know that the EATS is not homogeneous in brightness, but shows a ring-like structure, which means emission from the high latitude portion plays the dominant role in the afterglows (Waxman 1997; Sari 1998; Panaitescu & Mészáros 1998). At any time 2×10^4 s $< t < 2 \times 10^5$ s, although the central portion of the EATS is in the high density region so that the emission is very weak, the high latitude portion of the EATS, which dominates the afterglow emission, is still in the low density region (see Fig. 6) and the emissivity remains at a high level. So, the afterglow flux will not be affected too much by the density increase during this period. However, when $t \geq 2 \times 10^5$ s, the EATS passes through the density jump radius completely and the emissivity of the whole EATS becomes very low. The afterglow then naturally shows a steep decline. Secondly, the pulse-like rebrightening structure at exactly 2×10^4 s in the dashed line also leaves its fingerprint in the solid line. As a result, we can observe a shallow but clear rebrightening in the solid light curve beginning at the time of the density jump.

In reality, the density jump is usually due to the existence of a dense molecular cloud. Since molecular clouds can be magnetized, it is possible that ξ_B may be correspondingly much larger after the density jump in some cases. In Figure 7b, we assume that at the density jump radius, ξ_B increases by a factor of 50. This induces a prominent pulse-like structure in the dashed light curve where the EATS effect is not considered. When the EATS effect is included, the rebrightening is still very prominent. This mechanism may give an explanation to the marked rebrightenings observed in some GRB afterglows.

3.4 Energy Injection Cases

Evidence for prolonged activities of the central engines of GRBs has been found in a few events (Dai & Lu 2001; Zhang & Mészáros 2002; Björnsson, Gudmundsson & Johannesson 2004; Fan et al. 2004; Burrows et al. 2005; King et al. 2005; Watson et al. 2006). Here we assume that the kinetic energy of the GRB remnant increases instantly by a factor of 3 at $t = 2 \times 10^4$ s due to a sudden energy injection. The corresponding optical light curves are shown in Figure 8. Again we see that the effect of the EATS is to smooth down the variation in the light curve.

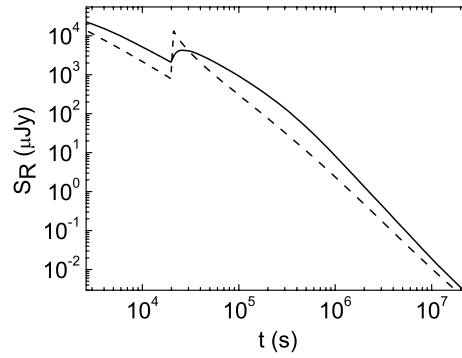


Fig. 8 *R*-band afterglow light curves of a “standard” jet in case of an energy injection occurring at 2×10^4 s. The energy supply is assumed to be completed instantly, and to increase the total kinetic energy of the GRB remnant by a factor of 3. The solid line is drawn including the EATS effect, and the dashed line, excluding the effect.

4 CONCLUSIONS AND DISCUSSION

In this article we study the EATS effect on GRB afterglows through numerical calculations. For isotropic fireballs and jets viewed on the axis, the inclusion of the EATS consideration generally does not change the shapes of the afterglow spectra and light curves; however, it does slightly harden the spectra, and postpone the peak time of the light curves. Also, the EATS effect tends to decrease the flux density before the peak, and to increase, after. The EATS effect is weaker in the X-ray bands than the optical frequencies.

When the GRB ejecta encounters a sudden density jump in the circumburst medium, the emissivity of the blastwave first rises rapidly, then decreases steeply to a much lower level due to the rapid deceleration of the shock in the denser environment. In this case, the EATS effect changes the afterglow light curve significantly, re-shaping the original pulse-like structure into a much weaker and more prolonged rebrightening. In the case of energy injection, EATS has a similar effect, i.e., smoothing down the light curve.

Our studies on the EATS effect have important implications on the observations. A good example is GRB 030329, for which a marked rebrightening was observed at $t \sim 1.6$ d in the optical afterglow (Lipkin et al. 2004). Huang, Cheng & Gao (2006) have reexamined this event numerically in the light of three models, namely, the density-jump model, the two-component jet model, and the energy-injection model. The EATS effect was considered in their calculations. They found that the energy-injection model is the most preferred choice for the rebrightening. However, even in their best fit to the optical afterglow with the energy-injection model, the theoretical rebrightening is still not rapid enough as compared with the observations, due to the EATS effect. This hints that we still need to seek other physical process for the rebrightening.

In the density jump case considered in our current study, there is a possibility that the portion of magnetic field energy (i.e., ξ_B) may also increase at the jump radius. This may happen when the density jump is caused by a magnetized molecular cloud. In this case, a prominent rebrightening is expected even if the EATS effect is taken into account. It is characterized by a rapid increase at the beginning and a steep decrease after the jump front completely passes through the EATS. This mechanism may give a natural explanation to the rebrightenings observed in some GRBs. For GRB 030329, it is quite probable that ξ_B might also change at the moment of the energy injection, which may have helped to contribute to the rebrightening. This possibility needs further check in the future.

Acknowledgements We thank the anonymous referee for helpful comments and suggestions. This research was supported by an RGC grant of the Hong Kong Government, and also partly supported by the National Natural Science Foundation of China (NSFC, Grants 10625313, 10233010, 10221001, 10573021 and 10433010), and the Foundation for the Author of National Excellent Doctoral Dissertation of P. R. China (Project No: 200125).

References

- Barthelmy S. D., Chincarini G., Burrows D. N. et al., 2005, *Nature*, 438, 994
Bianco C. L., Ruffini R., 2005, *ApJ*, 620, L23
Bjornsson G., Gudmundsson E. H., Johannesson G., 2004, *ApJ*, 615, L77
Burrows D. N., Romano P., Falcone A. et al., 2005, *Science*, 309, 1833
Costa E., Frontera F., Heise J. et al., 1997, *Nature*, 387, 783
Cusumano G., Mangano V., Chincarini G. et al., 2006, *Nature*, 440, 164
Dai Z. G., Huang Y. F., Lu T., 1999, *ApJ*, 520, 634
Dai Z. G., Lu T., 2001, *A&A*, 367, 501
Dai Z. G., Wu X. F., 2003, *ApJ*, 591, L21
Dermer C. D., Chiang J., Böttcher M., 1999, *ApJ*, 513, 656
Fan Y. Z., Wei D. M., Wang C. F., 2004, *MNRAS*, 351, L78
Fox D. B., Frail D. A., Price P. A. et al., 2005, *Nature*, 437, 845
Frail D. A., Kulkarni S. R., Nicastro S. R., Feroci M., Taylor G. B., 1997, *Nature*, 389, 261
Galama T. J., Groot P. J., van Paradijs J. et al., 1997, *Nature*, 387, 479
Gao T. T., Huang Y. F., 2006, *Chin. J. Astron. Astrophys. (ChJAA)*, 6, 305
Granot J., 2005, *ApJ*, 631, 1022
Granot J., Piran T., Sari R., 1999, *ApJ*, 513, 679
Haislip J., Nysewander M., Reichart D. et al., 2006, *Nature*, 440, 181
Hjorth J., Thomsen B., Nielsen S. R. et al., 2002, *ApJ*, 576, 113
Huang Y. F., Cheng K. S., 2003, *MNRAS*, 341, 263
Huang Y. F., Cheng K. S., Gao T. T., 2006, *ApJ*, 637, 873
Huang Y. F., Dai Z. G., Wei D. M., Lu T., 1998, *MNRAS*, 298, 459
Huang Y. F., Dai Z. G., Lu T., 1999, *MNRAS*, 309, 513
Huang Y. F., Dai Z. G., Lu T., 2000a, *MNRAS*, 316, 943
Huang Y. F., Gou L. J., Dai Z. G., Lu T., 2000b, *ApJ*, 543, 90
King A., O'Brien P. T., Goad M. R., Osborne E., Page K., 2005, *ApJ*, 630, L113
Kumar P., Granot J., 2003, *ApJ*, 591, 1075
Lazzati D., Rossi E., Covino S., Ghisellini G., Malesani D., 2002, *A&A*, 396, L5
Lipkin Y. M., Ofek E. O., Gal-Yam A. et al., 2004, *ApJ*, 606, 381
Mészáros P., Rees M. J., 1992, *MNRAS*, 257, 29P
Mészáros P., Rees M. J., 1997, *ApJ*, 476, 232
Moderski R., Sikora M., Bulik T., 2000, *ApJ*, 529, 151
Nakar E., Piran T., 2003, *ApJ*, 598, 400
Panaitescu A., Mészáros P., 1998, *ApJ*, 493, L31
Panaitescu A., Mészáros P., 1999, *ApJ*, 526, 707
Piran T., 2004, *Rev. Mod. Phys.*, 76, 1143
Price P. A., Cowie L. L., Minezaki T., Schmidt B. P., Songaila A., Yoshii Y., 2006, *ApJ*, 645, 851
Salmonson J. D., 2003, *ApJ*, 592, 1002
Sari R., 1998, *ApJ*, 494, L49
Sari R., Esin A. A., 2001, *ApJ*, 548, 787
Sari R., Narayan R., Piran T., 1996, *ApJ*, 473, 204
Sari R., Piran T., Narayan R., 1998, *ApJ*, 497, L17
Su C. Y., Qin Y. P., Fan J. H., Han Z. Y., 2006, *Chin. J. Astron. Astrophys. (ChJAA)*, 6, 323
Tagliaferri G., Antonelli L. A., Chincarini G. et al., 2005, *A&A*, 443, L1
Tam P. H., Pun C. S. J., Huang Y. F., Cheng K. S., 2005, *New Astron*, 10, 535
van Paradijs J., Kouveliotou C., Wijers R., 2000, *ARA&A*, 38, 379
Vietri M., 1997, *ApJ*, 488, L105
Villasenor J. S., Lamb D. Q., Ricker G. R. et al., 2005, *Nature*, 437, 855
Vreeswijk P. M., Galama T. J., Owens A. et al., 1999, *ApJ*, 523, 171
Watson D., Reeves J. N., Hjorth J. et al., 2006, *ApJ*, 637, L69
Waxman E., 1997, *ApJ*, 491, L19
Wei D. M., Lu T., 2000, *A&A*, 360, L13
Wijers R. A. M. J., Rees M. J., Mészáros P., 1997, *MNRAS*, 288, L51
Zhang B., 2007, *Chin. J. Astron. Astrophys. (ChJAA)*, 7, 1
Zhang B., Mészáros P., 2002, *ApJ*, 566, 712
Zhang B., Mészáros P., 2004, *Int. J. Mod. Phys. A*, 19, 2385